UNSTEADINESS IN A 2D CYLINDER WAKE FLOW AT MACH 6

Premika S. Thasu
Department of Aerospace Engineering
Indian Institute of Science
Bengaluru 560012
<premikat@iisc.ac.in>

Vaisakh Sasidharan
Department of Aerospace Engineering
Indian Institute of Science
Bengaluru 560012
<vaisakhs@iisc.ac.in>

Subrahmanyam Duvvuri
Department of Aerospace Engineering
Indian Institute of Science
Bengaluru 560012
<subrahmanyam@iisc.ac.in>

ABSTRACT

Flow oscillations in the near-wake of a 2D circular cylinder at Mach 6 are experimentally investigated. Time-resolved schlieren and wall-pressure measurements are analyzed to infer a coherent spatial structure and frequency (Strouhal number) for the oscillations. The findings presented here lend support to a universal scaling of Strouhal number proposed in recent literature for high-speed cylinder wakes.

INTRODUCTION

Blunt-body wake flows are a class of fluid dynamics problems that have received close research attention over the past several decades. A large proportion of the research effort has been in the low-speed (incompressible) flow regime, with the canonical 2D cylinder wake being a classic example (see for instance Williamson, 1996). Whereas the number of high-speed (compressible) wake flow studies is somewhat limited. Early efforts to understand the near-wake region in high-speed flows employed experimental wall-pressure measurements and hot wire anemometry (McCarthy Jr & Kubota, 1964; Dewey Jr, 1965), and were accompanied by development of low-order models (Chapman *et al.*, 1958; Reeves & Lees, 1965).

A primary understanding of the flow structure in the base and near-wake regions of a circular cylinder at hypersonic Mach numbers emerged from the experimental studies of McCarthy Jr & Kubota (1964) and Dewey Jr (1965). The schematic in figure 1 illustrates the key flow features in the wake of a 2D circular cylinder in a high-speed flow, and also shows a time-averaged schlieren intensity map obtained from the present experiments at Mach number $M_\infty = 6$ (detailed in the next section). The flow downstream of the leading bow shock wave, in the vicinity of the fore stagnation point, is subsonic. The fluid from this region accelerates as it moves around the cylinder, and attains supersonic Mach numbers downstream of the sonic line. A set of expansion fans in the aft region result in a further increase in Mach number as the flow curves around the cylinder. Unlike in an incompressible flow scenario where an adverse pressure gradient gets established in the aft region, the expanding flow yields a favourable pressure gradient, and hence it is natural to expect that the boundary layer would not be prone to separation. However, the downstream reattachment shock wave, which turns the flow parallel to the free-stream direction, causes a pressure jump. The elevated pressure is communicated upstream through the subsonic region and the boundary layer, thereby causing flow separation and the formation of a free shear layer. According to Dewey Jr (1965) the static pressure along the surface just upstream of the separation point is below the base pressure level, and then subsequently rises to the base pressure value through the self-induced pressure gradient that accompanies separation. Since the pressure rise required to separate the boundary layer is modest, the separation shock wave generated in the process is weak.

The dependence of near-wake features on the governing flow parameters, *i.e.* Mach and Reynolds numbers, was investigated in more recent studies and empirical correlations for the same were obtained (Park *et al.*, 2016; Hinman & Johansen, 2017; Grasso & Pettinelli, 1995; Lamb & Oberkampf, 1995). While the mean (temporal) flow structure of the near-wake region of a circular cylinder has been characterized in detail (McCarthy Jr & Kubota, 1964; Bashkin *et al.*, 2002; Park *et al.*, 2016), the unsteady character of the wake has received surprisingly little attention, with the work of Schmidt & Shepherd (2015) seemingly being the only exception. Experiments by Schmidt & Shepherd (2015) in a Mach 4 flow revealed periodic oscillations in the wake, with a Strouhal number behaviour over a decade range in the Reynolds numbers that suggests the free shear layer length to be the governing length scale for the oscillations. The present work aims to build on these observations and obtain a more detailed understanding of the unsteady flow dynamics in the near-wake of a circular cylinder at high speeds.

EXPERIMENTAL SET-UP

Experiments with a 2D circular cylinder in a Mach 6 flow were performed in the Roddam Narasimha Hypersonic Wind Tunnel (RNHWT) at IISc. RNHWT is a pressure-vacuum type 0.5 m diameter enclosed free-jet facility (see Sasidharan & Duvvuri, 2021, for further details on the wind tunnel). In

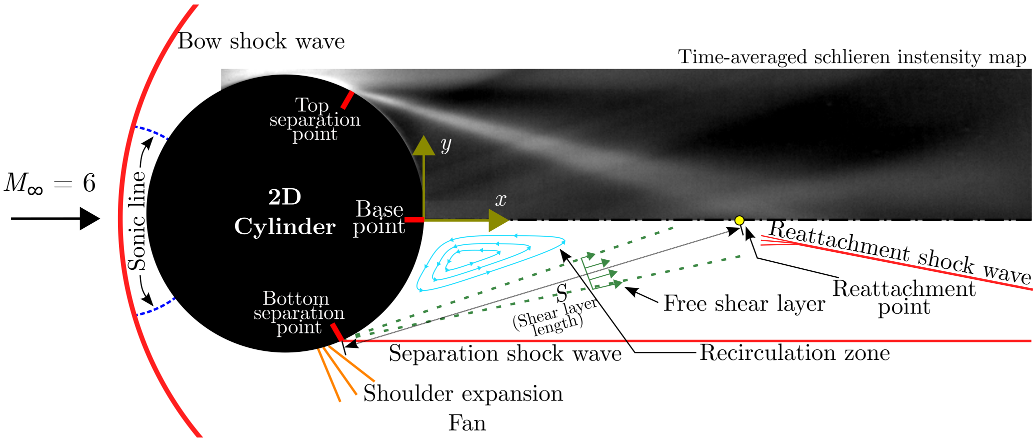

Figure 1: Key features of hypersonic flow past a 2D circular cylinder. The time-averaged schlieren intensity map, which was experimentally obtained, indicates density gradients in the direction normal to the free-stream flow.

these experiments the flow stagnation pressure and temperature were set to $P_0 = 9.7$ bar and $T_0 = 460$ K respectively. A test model of diameter D = 50 mm and span L = 120 mm was used in this study with provisions to install miniature pressure transducers on the span-wise mid-plane at the top and bottom separation points and the centerline base point; these locations are marked in figure 1. The Reynolds number with respect to the diameter of the cylinder (D) is defined as

$$Re_D = \frac{U_\infty D}{\nu_\infty}, \tag{1}$$

where U_∞ and ν_∞ are free-stream velocity and kinematic viscosity respectively. Re_D for the present study is 4.29×10^5.

High-speed schlieren data recorded at 100,000 frames per second was obtained in the near wake region of the cylinder; the schlieren set-up is similar to the one used earlier by Sasidharan & Duvvuri (2021). The schlieren "knife-edge" was set in horizontal position to capture density gradients normal to the free-stream flow direction, *i.e.* $\partial\rho\,/\,\partial y$. A high value of knife-edge cut off was used to obtain sufficient sensitivity to density gradients. This brings about a non-linearity in light intensity that breaks the symmetry between corresponding bright/dark bands in the top/bottom halves of the wake. This aspect is seen in figure 2a which shows an instantaneous schlieren snapshot of the flow. The top/bottom symmetry in the image is missing, with flow features that are clearly visible in the bright band (top half) not being captured equally well by the saturated dark bands (bottom half). However, given the physical symmetry, the flow is statistically similar in the top and bottom halves, and essential flow elements are contained in both the halves. It is noted that key flow features – separation shock wave, free shear layers, re-attachment shock wave – can be identified in the instantaneous schlieren snapshot of the flow. In addition to schlieren visualization, time-resolved pressure measurements were made at the top and bottom separation points and the base point using piezo-resistive transducers (Kulite XCE-093-5A) that were flush-mounted to the surface of the cylinder model. These transducers have a resonance frequency of 150 kHz, thereby limiting the usable bandwidth to about 30 kHz. The 30 kHz bandwidth however easily covers the frequency range of interest in these experiments. The transducers have a sensing diameter of 2.4 mm, and hence the pressure output from the transducers are to be interpreted as spatial averages over the corresponding circular area.

RESULTS AND DISCUSSION

The standard deviation map of temporal fluctuations in schlieren intensity shown in figure 2b highlights regions of the flow that have a high level of local unsteadiness. It is seen that the neck region, *i.e.*, the region where the top and bottom shear layers meet, and reattachment shock waves are unsteady. A small degree of local unsteadiness is also noted in the free shear layer close to the separation point. Schmidt & Shepherd (2015) analyzed the Fourier spectrum of local intensity fluctuations in the neck region and found that a single frequency can be associated with the unsteadiness. Here we use the modal analysis technique of spectral proper orthogonal decomposition (SPOD) to extract a timescale and associated spatial structure for the flow from the time-resolved schlieren data. The technique is briefly outlined below and results are presented.

Spectral proper orthogonal decomposition

SPOD is the frequency domain form of proper orthogonal decomposition (POD) and is suited for extracting physically-meaningful spatio-temporal coherent structures in statistically stationary flows (Towne *et al.*, 2018). SPOD finds an optimal orthogonal basis for the data such that a subset of the obtained modes capture a larger fraction of the total energy (variance) than any other orthogonal basis. The distinction between SPOD and standard POD is that SPOD modes are orthogonal under a space-time inner product, unlike POD modes that are only spatially orthogonal. Mathematically, SPOD modes are the eigenvectors of a cross-spectral density tensor at each frequency.

Consider a single time series consisting of N snapshots sampled at sampling frequency F_s broken into L blocks/realizations, each consisting of M snapshots. Let $q_j^{(k)}$ be the k^{th} realization of the vector of observations at discrete time t_j. The discrete temporal Fourier transform for each realization is written as

$$\widehat{q}_m^{(k)} = \sum_{j=0}^{M-1} q_{j+1}^{(k)} \mathrm{e}^{-\mathrm{i}2\pi jm/M} \quad \text{for} \quad m = -\frac{M}{2}+1, ..., \frac{M}{2}. \tag{2}$$

The corresponding power spectral density (PSD) for each re-

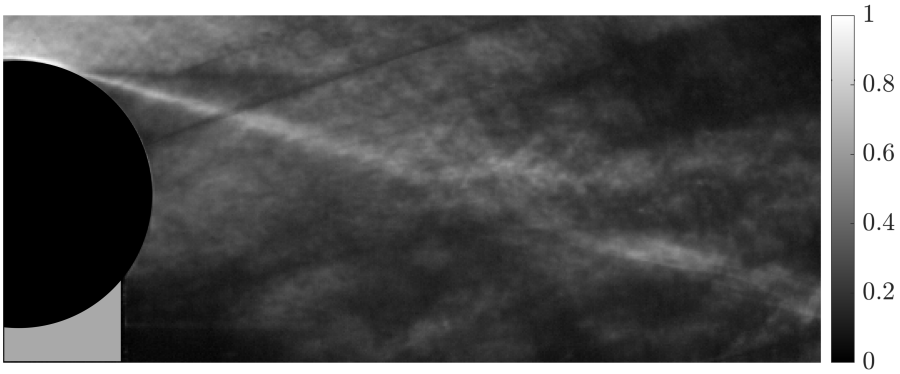

(a) An instantaneous schlieren snapshot with normalized intensity, which indicates density gradients in the direction normal to the free-stream flow.

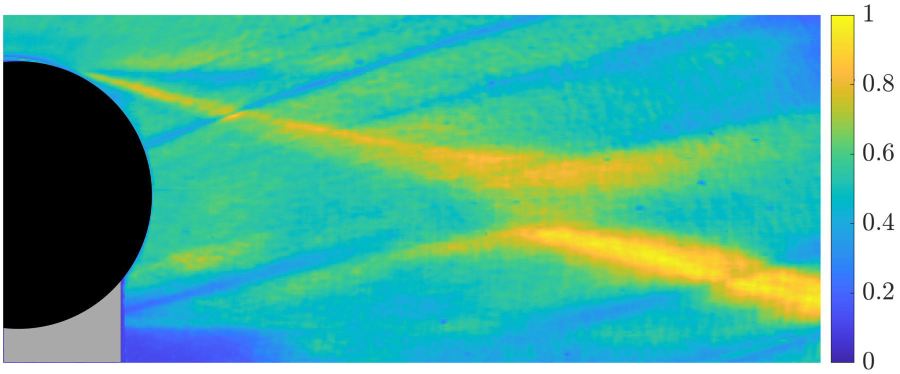

(b) Map of the normalized standard deviation of temporal fluctuations in schlieren intensity.

Figure 2: Schlieren of the near-wake region downstream of the cylinder.

alization, denoted by $\widehat{P}_m^{(k)}$, then follows from $\widehat{q}_m^{(k)}$ as

$$\widehat{P}_m^{(k)} = \frac{1}{N^2}\left|\widehat{q}_m^{(k)}\right|^2. \tag{3}$$

The rest of the analysis is performed at individual frequencies. The data matrix $\widehat{\boldsymbol{Q}}^{(m)}$ of size $P \times L$ corresponding to any one frequency is constructed such that each column corresponds to the PSD vector along P spatial points. The cross correlation matrix, $\widehat{\boldsymbol{S}}^{(m)}$, is written as

$$\widehat{\boldsymbol{S}}^{(m)} = \widehat{\boldsymbol{Q}}^{(m)}\widehat{\boldsymbol{Q}}^{(m)\mathrm{T}}, \tag{4}$$

and the eigenvalue decomposition of the cross-correlation matrix is carried out as

$$\widehat{\boldsymbol{S}}^{(m)}\boldsymbol{\Phi}^{(m)} = \boldsymbol{\Phi}^{(m)}\boldsymbol{\Lambda}^{(m)}. \tag{5}$$

Here $\boldsymbol{\Phi}^{(m)}$ is a size $P \times P$ matrix whose columns $\phi_p^{(m)}$ ($p = 1,2,...,P$) are the SPOD modes at a particular frequency $f_m = mF_s/M$, and $\boldsymbol{\Lambda}^{(m)}$ is the corresponding diagonal matrix whose elements are the eigen values $\lambda_p^{(m)}$.

Strouhal number and wall-pressure signature

SPOD was performed with schlieren data with $L = 13$, $M = 2048$, and $F_s = 100,000$. Figure 3 shows the modal en-

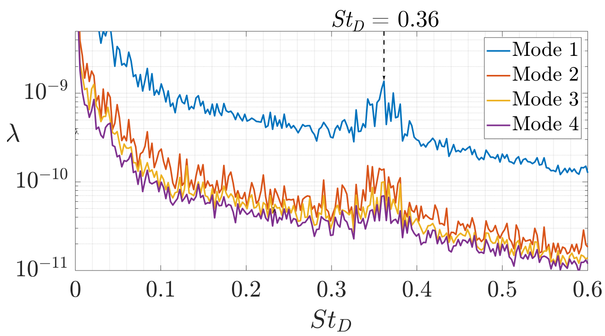

Figure 3: The modal energy spectrum of the first four modes obtained from SPOD. The dominant frequency corresponding to the oscillations can be identified as $St_D = 0.36$.

ergy spectrum λ of the first four modes thus obtained. The frequency f is shown in the form of a non-dimensional Strouhal number based on the cylinder diameter,

$$St_D = \frac{fD}{U_\infty}. \tag{6}$$

Mode 1 is clearly seen to be more energetic in comparison with the other modes, and hence any coherent spatial structures present in the flow are expected to be captured by this mode. Further, a peak in the spectrum is observed at $St_D = 0.36$ in the mode 1 spectrum, and spectra of other modes also reflect increased energy at the same Strouhal number. This analysis

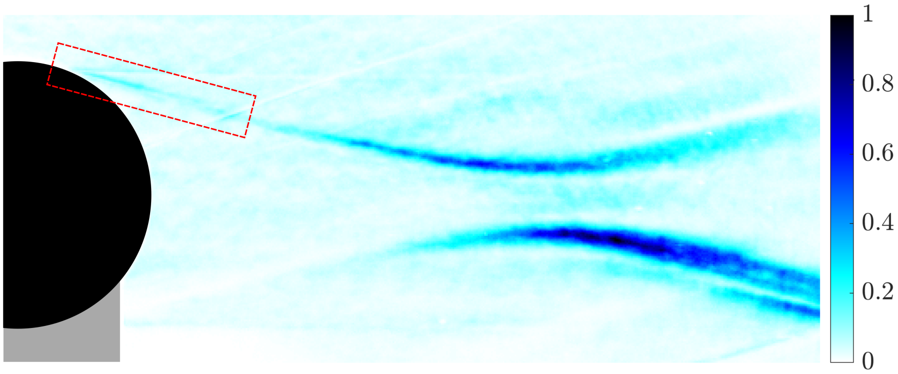

Figure 4: Amplitude map of SPOD mode 1. The red-colored bounding box highlights the upstream portion of the shear layer where a signature of energetic activity is visible.

suggests that the dominant oscillations in the near-wake region occur at a Strouhal number St_D of 0.36; figure 4 shows the spatial mode shape at this Strouhal number. For reference, $St_D = 0.36$ corresponds to a physical frequency of 6.49 kHz. The qualitative similarities between intensity maps shown figures 2b and 4 also suggests that the frequency corresponding to $St_D = 0.36$ is a significant driver of the overall flow unsteadiness. It is interesting to note that mode 1 shows a signature of fluctuations along the entire shear layer length; the upstream portion of the shear layer is highlighted with a bounding box in figure 4.

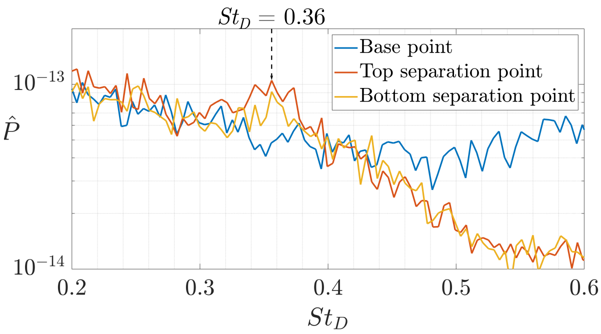

Figure 5: Power spectral density ($\widehat{P}$) of non-dimensional pressure (p/P_0) fluctuations at the top and bottom separation points and the base point.

Based on the SPOD results, we expect to see a footprint of the oscillation frequency at the separation points. Figure 5 shows the PSD curves of the non-dimensional pressure fluctuations p/P_0 measured at the top and bottom separation points and the base point. A peak is indeed seen at $St_D = 0.36$ in PSD curves of both top and bottom separation points. Interestingly, there appears to be no activity at that Strouhal number in the base region. The phase difference in the pressure signals between the top and bottom separation points at $St_D = 0.36$ was extracted from a cross power spectral density (CPSD) calculation, and was found to be very close to π radians. This suggests that disturbances from the top and bottom shear layers are out of phase as they arrive at the neck, and this perhaps is a key feature of the overall mechanism that governs the near-wake oscillations.

Schmidt & Shepherd (2015) had proposed a universal Strouhal number based on the length of the shear layer S (marked in figure 1),

$$St_S = \frac{fS}{U_\infty}, \tag{7}$$

and found St_S to be approximately 0.48 over the Reynolds number range $2 \times 10^4 < Re_D < 5 \times 10^5$ at $M_\infty = 4$. From the present experiment we find $St_S = 0.47$. The close match between the Strouhal numbers lends support to the universal scaling proposed by Schmidt & Shepherd (2015).

BRIEF CONCLUSIONS

The dynamics of the near-wake for a Mach 6 flow past a 2D circular cylinder was investigated experimentally through time-resolved schlieren and wall-pressure measurements (on the cylinder aft surface). A Strouhal number for coherent oscillations in the wake and associated spatial structure was obtained by applying spectral proper orthogonal decomposition to the schlieren data. The Strouhal number is close to the universal scaling proposed by Schmidt & Shepherd (2015) from experimental observations at $M_\infty = 4$. Schmidt & Shepherd (2015) hypothesize that propagation of acoustics waves between the separation points and the neck through the subsonic portion of the shear layer sustains the wake oscillations. The signature of oscillations seen at the separation points in the present experiments are consistent with the hypothesis. A more detailed study with stability calculations is needed to obtain a full understanding of the oscillations and the mechanisms involved in sustaining the same.

ACKNOWLEDGEMENTS

Support from GoI Ministry of Education PhD Scholarship (P.S.T.), SERB National Postdoctoral Fellowship (V.S. – file no. PDF/2020/001278), and Saroj Poddar Trust (S.D.) is gratefully acknowledged.

REFERENCES

Bashkin, V A, Vaganov, A V, Egorov, I V, Ivanov, D V & Ignatova, G A 2002 Comparison of calculated and experimental data on supersonic flow past a circular cylinder. *Fluid Dynamics* **37** (3), 473–483.

Chapman, D R, Kuehn, D M & Larson, H K 1958 Investigation of separated flows in supersonic and subsonic streams with emphasis on the effect of transition. *NACA Technical Report.* No. NACA–TR–1356.

Dewey Jr, C F 1965 Near wake of a blunt body at hypersonic speeds. *AIAA Journal* **3** (6), 1001–1010.

Grasso, F & Pettinelli, C 1995 Analysis of laminar near-wake hypersonic flows. *Journal of Spacecraft and Rockets* **32** (6), 970–980.

Hinman, W S & Johansen, C T 2017 Reynolds and Mach number dependence of hypersonic blunt body laminar near wakes. *AIAA Journal* **55** (2), 500–508.

Lamb, J P & Oberkampf, W L 1995 Review and development of base pressure and base heating correlations in supersonic flow. *Journal of Spacecraft and Rockets* **32** (1), 8–23.

McCarthy Jr, J F & Kubota, T 1964 A study of wakes behind a circular cylinder at M equal 5.7. *AIAA Journal* **2** (4), 629–636.

Park, G, Gai, S L & Neely, A J 2016 Base flow of circular cylinder at hypersonic speeds. *AIAA Journal* **54** (2), 458–468.

Reeves, B L & Lees, L 1965 Theory of laminar near wake of blunt bodies in hypersonic flow. *AIAA Journal* **3** (11), 2061–2074.

Sasidharan, V & Duvvuri, S 2021 Large- and small-amplitude shock-wave oscillations over axisymmetric bodies in high-speed flow. *Journal of Fluid Mechanics* **913**, R7.

Schmidt, B E & Shepherd, J E 2015 Oscillations in cylinder wakes at Mach 4. *Journal of Fluid Mechanics* **785**, R3.

Towne, A, Schmidt, O T & Colonius, T 2018 Spectral proper orthogonal decomposition and its relationship to dynamic mode decomposition and resolvent analysis. *Journal of Fluid Mechanics* **847**, 821–867.

Williamson, C H K 1996 Vortex dynamics in the cylinder wake. *Annual Review of Fluid Mechanics* **28** (1), 477–539.